# Supplementary Online Content

Zeppenfeld DM, Simon M, Haswell JD, et al. Association of perivascular localization of aquaporin-4 with cognition and Alzheimer disease in aging brains. *JAMA Neurol*. Published online November 28, 2016. doi:10.1001/jamaneurol.2016.4370.



This supplementary material has been provided by the authors to give readers additional information about their work.

**eMethods**

*Human tissue*

At the time of autopsy, brain tissue from several regions, including a systematic dissection of the middle frontal gyrus was frozen for biochemical analysis and fixed for histological assessment. After fixation for at least 10 days in neutral buffered formalin, brain tissue was dissected, processed into paraffin blocks using standard histologic techniques, and 6-micron paraffin sections were prepared.

*Neuropathological evaluation*

Brains in the Oregon Brain bank undergo neuropathologic assessment for Aβ plaque density and neurofibrillary pathology at the time of autopsy based on established criteria. Aβ plaque density was evaluated based on the four point (0-3) Consortium to Establish a Registry for AD (CERAD) neuritic plaque score (corresponding to no neuritic plaques or sparse, moderate, or frequent plaques, respectively), while Braak staging was used to score neurofibrillary pathology[1-3]. No subjects exhibiting neocortical or midbrain Lewy bodies, hippocampal sclerosis, macroscopic infarction, or other non-Alzheimer's disease pathologic findings were selected from the Oregon Brain Bank cohort for evaluation in the present study.

Among subjects undergoing histological evaluation of AQP4 expression and localization, cortical vascular pathology was evaluated by a neuropathologist (MRG). For assessment of vascular injury, sections of frontal cortex with subcortical white matter were stained with luxol fast blue/PAS and/or hemotoxylin and eosin, and sections of

occipital cortex were stained with Congo Red. The slides were coded and examined without knowledge of study group. Sections were rated on a 4-point ordinal scale (0-3) on the degree of arteriolosclerosis, perivascular hemosiderin leakage, perivascular space dilation, and myelin loss in the frontal cortex and cortical amyloid angiopathy in the occipital cortex according to the criteria published by Deramecourt et al.[4]. The scores for each category were combined to give a total vascular injury score (VIS), with a maximum score of 15.

*Western blot*

Grey matter tissue was collected from frozen frontal gyrus autopsy samples. Tissue was then homogenized in extraction buffer (250mM Sucrose, 60mM KCL, 15mM Tris HCl, 15mM NaCl, 5mM EDTA, 1mM EGTA) containing protease inhibitors. The membrane fraction was then isolated by standard centrifugation protocol. Briefly, homogenate was spun at 2000 g for 10 min at 4°C. The supernatant was collected, then spun again at 17,000 g for 20 min at 4°C. The resulting pellet was re-suspended in extraction buffer. Samples were stored at -80°C until quantified via by Western blot.

Membrane protein was denatured with SDS-PAGE and boiling, then 5 µg was loaded into a Bis-Tris gel (Invitrogen Nu-Page 4-12%), and run at 200 mV for 90 minutes at 4°C. Gels were then transferred to a PVDF membrane at 30 mV for 60 minutes at 4°C. Membranes were blocked with 5% milk in phosphate buffered saline (137 mM NaCl, 2.7mM KCl, 10 mM $Na_2HPO_4$, 2 mM $KH_2PO_4$) plus .05% Tween 20 (PBST) for 1 hour at room temperature before being incubated overnight at 4°C with primary antibody

against AQP4 diluted in 5% milk/PBST (1:500, Millipore rabbit polyclonal, AB3594). Membranes were washed in PBST, then incubated with a horseradish-peroxidase conjugated secondary antibody to rabbit immunoglobulin (1:1000, GE Healthcare Life Sciences) for 4 hours at 4°C. Membranes were then washed with PBST again, and the chemiluminescent signal was generated by washing with a chemiluminescent substrate. To detect β-actin, blots were stripped for 10 minutes with Restore Stripping Buffer (Thermo 21059), then the above steps were repeated with primary antibody against β-actin (1:1000, Sigma mouse monoclonal A5441) and horseradish-peroxidase conjugated secondary antibody to mouse immunoglobulin (1:1000, GE Healthcare Life Sciences). Chemiluminescence was detected with an Alpha Innotech Multi-Image II light cabinet. Densitometry of bands was performed using Fiji software. To measure fluorescent intensity, a region of interest (ROI) was defined as the minimum sized rectangle necessary to measure the largest band. Mean fluorescent intensity was then collected. The top band was defined as AQP4-M1 and the bottom band was defined as AQP4-M23. Background fluorescence was subtracted from measured values, and both AQP4-M1 and AQP4-M23 were normalized by dividing the AQP4 value by the β-actin value. To derive the ratio of AQP4-M23:AQP4-M1, the normalized value of AQP4-M23 was divided by the normalized value of AQP4-M1.

*Immunofluorescence and image analysis*

Frontal cortex sections 6 microns thick were deparaffinized, incubated in 10% formic acid for 10 minutes, then heated in 0.5 mM citric acid at pH 6.0 for 30 minutes for

antigen retrieval. All rinses were with Tris-buffered saline, pH 7.6 with 0.1% Triton X-100. Sections were incubated with 3% normal donkey serum in phosphate buffered saline with 1% BSA and 0.1% Triton X-100 (blocking solution) for 20 minutes at room temperature. Sections were incubated with the primary antibodies (rabbit anti-AQP4, Millipore #AB3594, 1:800; mouse anti-GFAP, Millipore #MB360, 1:500; mouse anti-$A\beta_{1-42}$, Covance #SIG-39142, 1:800) diluted in blocking serum overnight at 4°C. Fluorescent conjugated secondary antibodies (rhodamine donkey anti-rabbit, Jackson #711-295-152, 1:400 for AQP4; Cy2 donkey anti-mouse, Jackson #715-225-150, 1:400 for GFAP) or biotinlyated horse anti-mouse 1:200 for $A\beta_{1-42}$ (Vector #BA-2000) were applied for 150 minutes at room temperature. The biotinylated secondary antibody was visualized with Cy2 streptavidin, 1:400 (Amersham #PA42001). Sections were counterstained with Hoechst 33342 (Molecular Probes, 1:3000) and cover slipped with Prolong Anti-Fade Gold reagent (Life Technologies).

Quantification of AQP4-IR and perivascular AQP4 localization employed an imaging and analysis process adapted from approaches our group has previously used to evaluate AQP4 localization in rodent tissue[5-7]. 2.2 x 4.6 mm segments of tissue extending from the pial surface to the subcortical white matter were captured in each of three fluorescence channels at 20X objective power on a Nikon A1R+ resonant scanning confocal microscope. These images were wide-field, two-dimensional montages generated in an automated manner by the Nikon Elements software package. All image analysis was conducted by blinded evaluators with FIJI software through a workflow shown in **eFigure 4**. For evaluation of global AQP4-IR and perivascular AQP4 localization, the wide-field montage was divided into a grid of 192 µm x 192 µm

subregions. A random sampling of subregions representing 20% of the wide-field montage area were selected and analyzed. To evaluate global AQP4-IR, mean fluorescence intensity within the AQP4 channel was measured and averaged across all subregions for each subject. To evaluate perivascular AQP4 localization, 3-7 capillaries (3.5-6 μm in diameter) were identified within each subregion by the absence of tissue autofluorescence circumscribed by enriched GFAP immunoreactivity and elliptical nuclei. Mean perivascular fluorescent intensity was measured within 3.1 μm (5 pixel) wide, donut-shaped ROIs spanning each capillary and its perivascular space (e**Figure4**). The ratio of the mean fluorescent intensity in the perivascular ROI to the global AQP4-IR was taken as a measure of perivascular AQP4 localization within a subregion, with a greater ratio reflecting greater localization of AQP4 to perivascular domains. Values were averaged across all subregions to define perivascular AQP4 localization for each subject. A median of 196 (range = [120 – 273]) vessels from a median of 46 (range = [26 - 60]) subregions were analyzed per subject to quantify perivascular AQP4 localization.

*Statistical Methods*

Covariate balance between Young, Aged and AD groups was evaluated using Chi-square testing for discrete factors (gender) while mean differences in continuous covariates (age, years of schooling, post-mortem interval, and measures of AQP4 expression and localization) were compared among groups using either two-independent sample t-tests (specifically contrasting Aged controls versus AD subjects) or one-way ANOVAs with Tukey HSD pairwise comparisons across all three groups. Median comparisons for nonparametric variables Aβ plaque density, Braak stage and vascular injury score (VIS)) were carried out using either the Mann-Whitney test (specifically contrasting Aged

controls versus AD subjects) or the Kruskal-Wallis test across all three groups with multiple pairwise comparison testing carried out using Dunn's test. Regression analysis among the continuous outcomes (including age, Aβ plaque density, Braak stage, and measures of AQP4 expression and localization) assessed simple correlations using either Pearson's correlation coefficient (r) or Spearman's rank order correlation (rho). Subsequent analysis of the confounding effect of age on the outcomes of interest entailed covariate-corrected multiple OLS regression. When assessing the categorization of cognitive status, logistic regression was used to evaluate the predictive ability of the measures of interest to identify an aged subject as cognitively intact versus AD while correcting for confounding predictors such as age. A common concern with the data were violations of typical paramteric assumptions, specifically heteroskedascity across the AQP4 outcomes. For that reason, all one-way ANOVA's were adjusted using Welch's correction for inconsistent variance while all regression models (both ordinary least-squares and logistic) had their variance-covariance matrices adjusted by the Huber-White method to correct for inconsistent variance. Models corrected by heteroskedascity are indicated within the manuscript. For all regression models, standard residual analyses were used in order to verify regression model assumptions of homoscedasticity, multivariate normality and lack of colinearity. Multiple comparisons corrected p-values, means and standard errors of the mean are indicated in the manuscript with goodness-of-fit indicated by adjusted $R^2$. All statistical analyses were carried out using Prism 6 (GraphPad) and R 3.2.1[8].

**eTable 1. Vascular pathology of samples undergoing histological analysis.**

| | n | Vascular Injury Score (VIS, 0 – 15) | Arteriolo-sclerosis (0 – 3) | Cortical AA (0 – 3) | PV Hemosiderin (0 – 3) | PV Space Dilation (0 – 3) | Myelin Pallor (0 – 3) |
|---|---|---|---|---|---|---|---|
| **Young (<60 yrs)** | 10 | 2.5 (1.8 – 4.8) | 0.0 (0.0 – 0.5) | 0.0 (0.0 – 0.0) | 1.0 (0.0 – 3.0) | 1.0 (1.0 – 2.0) | 0.0 (0.0 – 0.3) |
| **Aged (>60yrs)** | 15 | 6.0 (5.0 – 7.0) | 1.0 (0.3 – 2.0) | 0.0 (0.0 – 0.5) | 2.0 (1.3 – 3.0) | 1.0 (1.0 – 2.0) | 1.0 (1.0 – 1.0) |
| **Alzheimer's Disease (>60yrs)** | 18 | 7.0 (6.0 – 8.8) | 2.0 (1.0 – 2.0) | 0.5 (0.0 – 2.0) | 2.0 (1.0 – 3.0) | 1.0 (1.0 – 1.8) | 1.0 (1.0 – 2.0) |

Values are median (inter-quartile range). Cortical amyloid angiopathy (AA); Perivascular (PV).

**eFigure 1. Post mortem interval is not associated with altered AQP4 expression or localization. (A-B)**

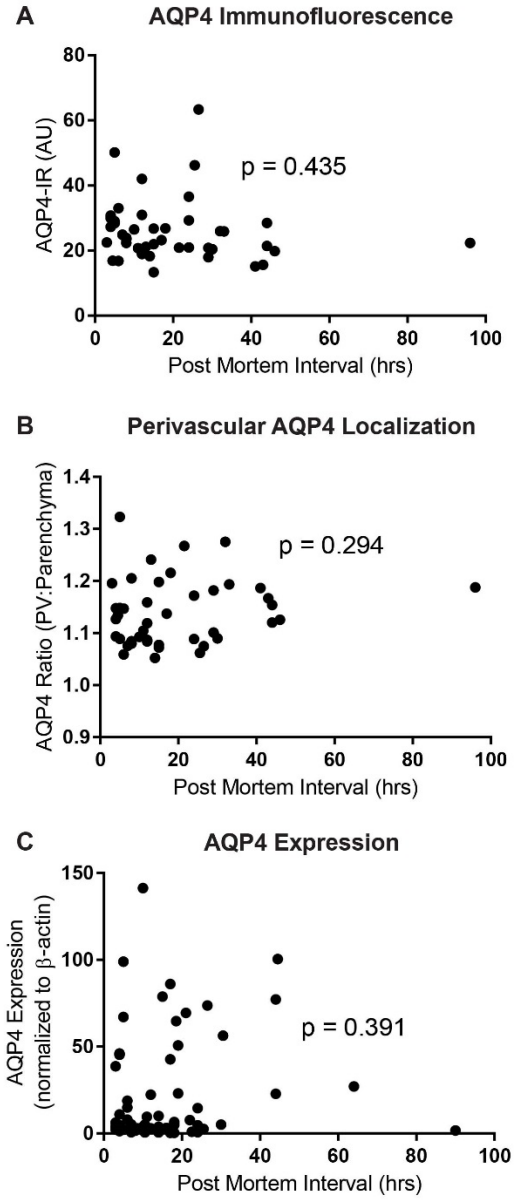


Among subjects undergoing immunofluorescence evaluation of AQP4 expression and localization, values were plotted versus post mortem interval. No significant association was observed between post mortem interval and AQP4-IR **(A**; p = 0.435, Pearson's correlation) or perivascular AQP4 localization (**B**; p = 0.294, Pearson's correlation). **(C)**

Among subjects undergoing evaluation of AQP4 expression by Western blot, AQP4 expression was plotted versus post mortem interval. No significant association was observed between AQP4 expression and post mortem interval ($p = 0.391$, Pearson's correlation).

**eFigure 2. Cortical vascular pathology is increased in the aging brain.**

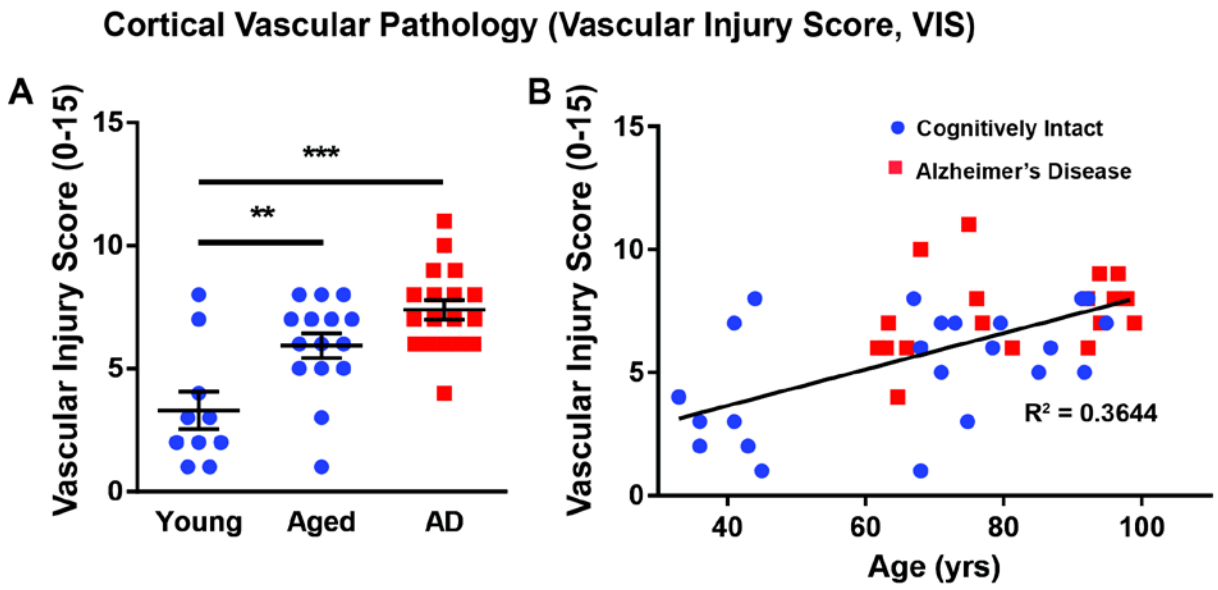


Cerebral vascular pathology was evaluated based on the criteria defined by Deramecourt et al.[4]. **(A)** Vascular pathology (Vascular Injury Score, VIS) was significantly increased in both the cognitively-intact Aged and AD subjects compared to Young subjects (**$p_{adj}$ = 0.038, ***$p_{adj}$ < 0.001; Kruskal-Wallis Test). **(B)** VIS was significantly associated with increasing age ($p < 0.001$, Pearson's correlation).

**eFigure 3. Reduced ratio of AQP4-M1 to AQP4-M23 expression in the aging and Alzheimer's disease brain.**

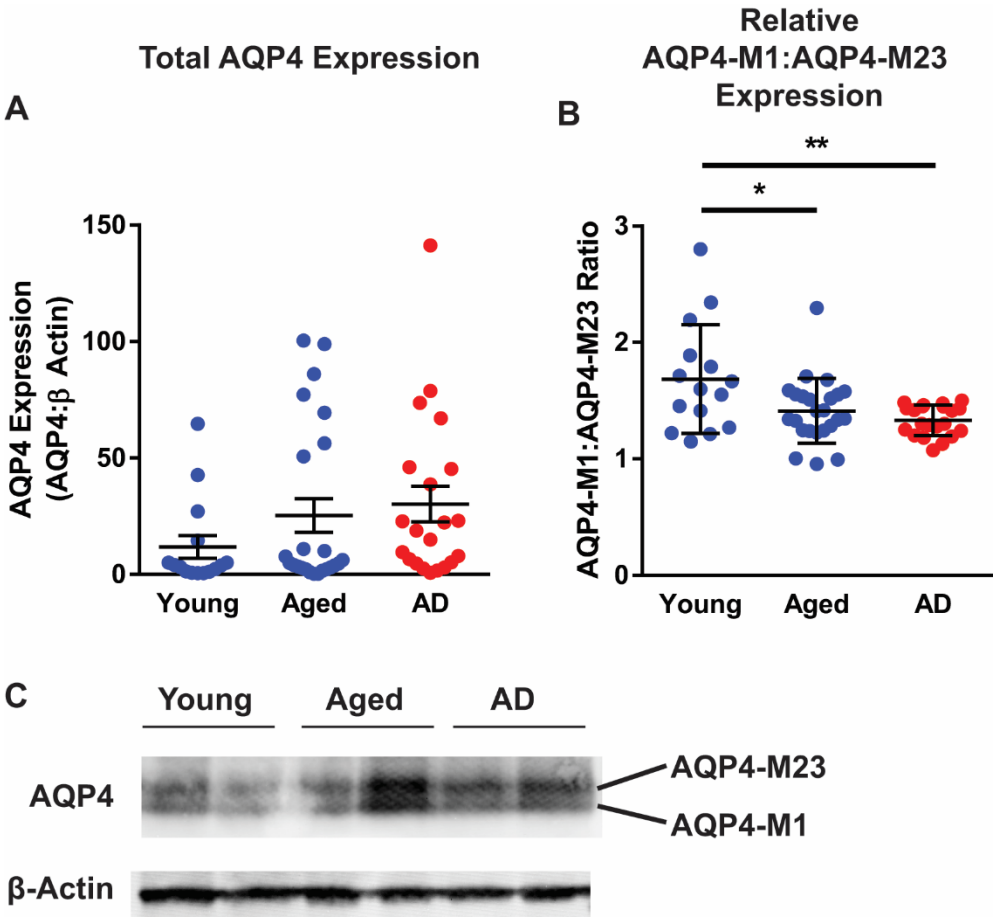


Total AQP4, AQP4-M1 and AQP4-M23 expression in frontal cortex were evaluated by Western blot. **(A)** No significant differences were observed in total AQP4 expression between Young, Aged or AD subjects. **(B)** Compared to Young subjects, the ratio of AQP4-M1:AQP4-M23 expression was significantly reduced in Aged and AD subjects (*$p_{adj}$ = 0.047, **$p_{adj}$ = 0.0085; Welch-corrected 1-way ANOVA). **(C)** Representative Western blot showing bands for AQP4-M1 and AQP4-M23 isoforms in Young, Aged and AD subjects.

**eFigure 4. Analysis of AQP4-IR and perivascular AQP4 localization**.

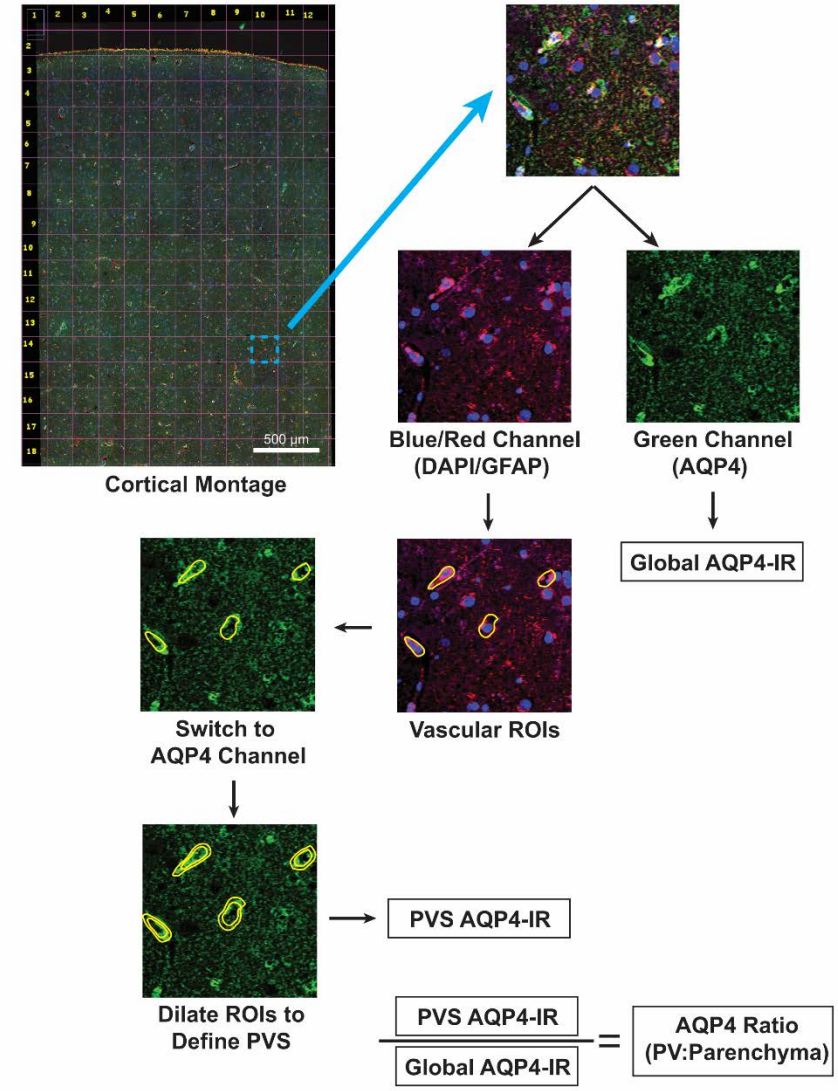


Systematic image analysis of Global AQP4-IR and AQP4 localization. **(A)** 192x192um sub-regions were randomly selected from a wide-field confocal cortical montage. **(B)** The mean intensity of the AQP4 channel was taken as a measurement of Global AQP4-IR. **(C)** 5-pixel "donut" Perivascular Space ROIs spanning the perivascular space were placed around Blood Vessels, which were identified by the absence of tissue autofluorescence circumscribed by enriched GFAP immunoreactivity and elliptical

nuclei. **(D)** The ratio of the Perivascular Space ROIs to Global AQP4-IR was used as a metric to quantify perivascular AQP4 localization. An average of 230 vessels from an average of 46 sub-regions were used to determine a subject's AQP4 localization.

**eReferences**


1. Montine TJ, Phelps CH, Beach TG, et al. National Institute on Aging-Alzheimer's Association guidelines for the neuropathologic assessment of Alzheimer's disease: a practical approach. *Acta neuropathologica.* 2012;123(1):1-11.
2. Hyman BT, Phelps CH, Beach TG, et al. National Institute on Aging-Alzheimer's Association guidelines for the neuropathologic assessment of Alzheimer's disease. *Alzheimer's & dementia : the journal of the Alzheimer's Association.* 2012;8(1):1-13.
3. Mirra SS, Heyman A, McKeel D, et al. The Consortium to Establish a Registry for Alzheimer's Disease (CERAD). Part II. Standardization of the neuropathologic assessment of Alzheimer's disease. *Neurology.* 1991;41(4):479-486.
4. Deramecourt V, Slade JY, Oakley AE, et al. Staging and natural history of cerebrovascular pathology in dementia. *Neurology.* 2012;78(14):1043-1050.
5. Kress BT, Iliff JJ, Xia M, et al. Impairment of paravascular clearance pathways in the aging brain. *Ann Neurol.* 2014;76(6):845-861.
6. Ren Z, Iliff JJ, Yang L, et al. 'Hit & Run' model of closed-skull traumatic brain injury (TBI) reveals complex patterns of post-traumatic AQP4 dysregulation. *J Cereb Blood Flow Metab.* 2013;33(6):834-845.
7. Wang M, Iliff JJ, Liao Y, et al. Cognitive deficits and delayed neuronal loss in a mouse model of multiple microinfarcts. *J Neurosci.* 2012;32(50):17948-17960.
8. *R: A Language and Environment for Statistical Computing* [computer program]. Vienna, Austria: R Foundation for Statistical Computing; 2013.